Received: 22 June 2022 | Revised: 13 October 2021 | Accepted: 19 October 2021

DOI: 10.1002/acm2.13468

JOURNAL OF APPLIED CLINICAL MEDICAL PHYSICS

REVIEW ARTICLE

Improving radiation physics, tumor visualisation, and treatment quantification in radiotherapy with spectral or dual-energy CT

Matthijs Ferdinand Kruis

Clinical Science CT, Philips Healthcare, Best, The Netherlands

Correspondence
Matthijs Ferdinand Kruis, Clinical Science CT, Philips Healthcare, Best, The Netherlands.
Email: matthijs.kruis@philips.com

[Correction added on Nov 22, 2021 after first online publication: Conflict of Interest and Section numbering have been updated]

Abstract

Over the past decade, spectral or dual-energy CT has gained relevancy, especially in oncological radiology. Nonetheless, its use in the radiotherapy (RT) clinic remains limited. This review article aims to give an overview of the current state of spectral CT and to explore opportunities for applications in RT.

In this article, three groups of benefits of spectral CT over conventional CT in RT are recognized. Firstly, spectral CT provides more information of physical properties of the body, which can improve dose calculation. Furthermore, it improves the visibility of tumors, for a wide variety of malignancies as well as organs-at-risk OARs, which could reduce treatment uncertainty. And finally, spectral CT provides quantitative physiological information, which can be used to personalize and quantify treatment.

KEYWORDS

conventional CT, dose calculation, dual-energy CT, material decomposition, proton therapy, quantification, radiotherapy, tumor visibility, spectral CT

1 | INTRODUCTION

Computed tomography (CT) has been around for over four decades and is indispensable in radiology. In 1983, the use of CT for radiotherapy (RT) treatment planning was first proposed,[1] and since then CT gained a pivotal role within RT treatment simulation. Most contemporary RT departments have a dedicated CT system used as a RT simulator. The anatomical information from CT supports delineation of the treatment target and organs-at-risk (OAR), while the attenuation information serves dose calculation purposes.

CT techniques have developed significantly over the years, with spectral CT imaging being one of the most prominent recent innovations. Conventional CT reports the averaged attenuation of a polychromatic radiation beam in the patient, which makes the measurements dependent on tube output and body size due to beam hardening.[2] However, since body attenuation of kilovoltage (kV) radiation is caused for over 85% by Compton scatter (CS) and the photoelectric effect (PE),[3] a much more quantitative dataset can be created through dual-energy (DE) CT.

By acquiring CT data at two different energy levels and decomposing these into two base images that can be used to describe the X-ray interaction (such as CS/PE or effective atomic numbers [Z_{eff}]/electron density [ED]), a quantitative dataset can be composed.[4] These datasets can be recomposed into other quantitative maps like virtual monochromatic images (VMI) representing mono-energetic photon energies at different kiloelectron Volt (keV) levels or single material decompositions,[5]

Initial decomposition can be done either in the image or in the sinogram domain. Decomposition in the image domain is the simplest solution, but since the reconstructions of the original input conceive conventional data, beam hardening artefacts are introduced during

reconstruction. It is therefore beneficial to perform decomposition in the sinogram domain before reconstruction,[6] although this requires a higher degree of spatial and temporal fidelity of the input data.[7] Decomposition can also be integrated into the reconstruction to further improve performance,[8] but this has not yet been implemented commercially due to significant increases in reconstruction time.

The concept of spectral CT was already described by Hounsfield in his seminal article from 1973.[9] However, computational limitations and a lack of integrated solutions hindered clinical implementation. In the last decade, spectral CT has become more mainstream, with various commercial implementations.[10]

The first available spectral technique was a sequential DE CT scan. By making two sequential scans with different tube potentials, a DE dataset can be created without any technical adaptations to the scanner.[11]

The technique is associated with a temporal offset in the order of a single scan duration, which poses a problem in the presence of (involuntary) motion and dynamic contrast enhancement and limits the possibility to perform spectral decomposition on sinogram data.[6] Also, integration with more complex acquisition protocols such as 4D CT is possible,[12] but it remains challenging to minimize motion artifacts.

A particular type of sequential DE CT is split-beam DE CT.[13] In a helical scan with a pitch under 0.5, a two-material filter allows for separation of the tube output into two separate energy levels. This technique allows for reduction of the temporal offset in comparison to sequential DE CT, but at the cost of spectral separation.[14]

Because of the limited temporal resolution and image quality, the use of sequential DE CT remained limited to certain niche applications,[15] such as urinary calculi,[16] gout,[17] and hepatic steatosis.[18] For RT, the use of these techniques is mainly limited to proton stopping power ratio (SPR) calculations.[19,20] It was only with the introduction of modern CT scanners providing integrated dose-neutral solutions with high image quality that spectral CT became an established technique in radiologic departments.[21]

The first integrated iteration introduced an extra X-ray source and detector pair. This technique allows for two simultaneous acquisitions at different kilovoltage peak (kVp) levels,[22] but the angular offset will introduce an effective temporal offset in sinogram space of 25% of the rotation time. This offset can cause motion uncertainties and will introduce a geometrical offset in helical mode, which makes sinogram-based decompositions challenging.[7] An additional limitation of a dual-source solution is that both detectors are competing for angular space.[22] This implies an intrinsic limitation to the spectral field-of-view (FOV), which is problematic for dose planning.[12]

Another implementation rapidly switches the tube potential during gantry rotation,[23] resulting in two scans with different energy levels. The advantage of this technique is that the temporal and geometrical offset between the scans is minimal, allowing sinogram-based decomposition.[7] However, this design poses a constraint on dose modulation, rotation speed, and scan speed to counteract for low energy flux which compromises the advantages over conventional CT.[24]

The most recent commercial iteration separates the signal by means of a dual-layer detector.[25] The top layer of the detector attenuates and detects the low-energy photons, while the bottom layer detects the remaining high-energy photons. A detector-based solution avoids acquisition constraints and creates two energy datasets without any offset. It has a reduced spectral separation in comparison to other solutions,[26] but with a spectral signal-to-noise ratio (SNR) that was at least comparable to other commercial solutions.[27] A unique feature of this technique is that by recombining the signal from the two layers, a conventional CT scan can be created from the spectral data at the energy level of the acquisition (120 or 140 kVp), which facilitates direct comparison and adoption.

The term spectral CT and DE CT are often interchanged. In this article the term spectral CT has been chosen, since it is more general than DE-CT and could also refer to other solutions like photon-counting (PC) CT. Photon counting CT detects individual photons and measures their energy.[28] This has the potential to provide CT data without electronic noise, improved tissue contrast, and improved image resolution.

Spectral CT imaging is gaining relevancy in the radiological clinic, since it improves image quality due to increase of image contrast[27] and a reduction of beam-hardening,[6] image noise[29] and metal artifacts.[30] Furthermore, it allows for quantification of the concentration of contrast agents such as iodine.[31] This is especially relevant for oncological application, since intravascular iodine is often used as a contrast agent for visualizing hyper- and hypo-perfusing tumors. By assessing spectral images such as low-keV VMI, virtual non-contrast (VNC), and iodine concentration images, iodine contrast is enhanced and quantifiable, which helps in the detection and assessment of tumors, lymph nodes, and metastasis.[32]

The increased use of spectral CT in oncological radiology has sparked an interest within the radiation oncology community.[33] However, despite having a potential in improved visualization and characterization of cancer,[32] most of the past works in radiation oncology focused on improving dose calculation for brachytherapy and proton therapy.

The main purposes of this review article are to increase the radiation oncology community's knowledge in latest usage of spectral CT and encourage novel clinical applications. This review addresses the threefold

benefits of spectral CT for RT, summarizing current and potential applications of spectral CT in the RT setting: improved dose calculation through reliable radiation physics, treatment certainty through improved disease visibility, and personalized treatment through physiological quantification.

2 | IMPROVED DOSE CALCULATION THROUGH RELIABLE RADIATION PHYSICS

Spectral CT measurements are more quantitative than measurements from conventional CT. Conventional CT reports the integral attenuation of a spectrum of radiation through the body, with results that are dependent on tube output and affected by beam hardening.

Spectral CT can provide a wide variety of well-defined results such as VMI, Z_{eff} and ED maps.[10] These results are in principle independent on scanner parameters and (in case of sinogram decomposition) not associated with beam hardening, although residual errors may persist.[6]

The implementation of spectral CT data as a replacement of the conventional planning CT for dose planning can improve accuracy for different RT modalities and potentially reduce the need for phantom calibration to convert Hounsfield units (HUs) into ED values.[34]

2.1 | Dose calculation improvements

The use of HU images from conventional CT is adequate for the estimation of the tissue attenuation in external beam RT with megavoltage (MV) photons, because attenuation in water for both MV[35] and kV beams[36] is mainly attributed to CS through ED. The large dose penumbra associated with MV external beam RT makes additional uncertainties less influential.[37] However, dose delivery techniques with a steeper dose gradient, such as brachytherapy[38] and proton therapy,[39] require more precise modeling for optimal therapy planning.

2.2 | Monte carlo simulations for brachytherapy

One of the first spectral applications described for RT was to use spectral CT for Monte Carlo simulations for brachytherapy.[38] For (low-energy) brachytherapy, the attenuation contribution of the PE and to a lesser extent Rayleigh scatter is much more prominent than for MV external beam RT. This makes the dose gradient sharper, thus also raising the need for quantification of the effective atomic number (Z_{eff}) for precise dose calculations.[40]

Moreover, Monte Carlo simulation is in general more sensitive to correct modeling of physical properties of tissues than classical dose calculation with analytical methods, requiring detailed knowledge of the atomic composition of the underlying tissue.[41] For this reason, most Monte Carlo techniques rely on organ tissue segmentations, with assumptions on the chemical makeup of each tissue type.

A method for classification of tissue groups based on conventional HU value ranges has been described by Schneider,[42] and this technique has since been regarded as the gold standard. However, studies have demonstrated that conventional CT segmentations are associated with large uncertainties, due to materials having similar conventional CT values, but different physical properties, leading to large dose calculation errors.[43] Spectral CT could improve these segmentations (see the section on visibility), and one study demonstrated that this could reduce local dose errors from +9% down to ±4% in brachytherapy with ^{103}Pd.[44]

However, segmentations based on HU values do not account for interpatient variations in tissue composition, especially in the case of local tumor pathology. Therefore, direct parametrizations of spectral features like ED and Z_{eff} to model elemental mass fractions have been proposed for particle therapy.[45] However, Z_{eff} is not a reliable quantity to reproduce the attenuation for tissues at energies under 50 keV, which poses challenges for modelling low-energy brachytherapy.[46] Therefore, other authors have proposed other models, like a three-material water-lipid-protein decomposition,[47] or a naive model with virtual materials through a linear model[48] or principle component analyses.[41] The impact of the latter technique on dose distribution was tested for brachytherapy and proved to give higher accuracy than a conventional CT solution.[49]

2.3 | Particle treatment planning

Particle therapy has a much steeper dose delivery curve than conventional external photon therapy, due to the associated Bragg peak.[39] This allows for more precise targeting, but also raises the bar for SPR estimation. Proton SPR estimations on conventional CT are associated with range uncertainties of 3%–3.5%.[50] For photon therapy such uncertainties in attenuation would constitute local dose variations under 1%,[37] but for proton therapy variations in SPR could lead to much larger dosimetric uncertainties due to dose shifts. Some studies report variations up to 7.8% with an average uncertainty of 2.1%,[20] although in theory differences could be up to 100% due to a local dose shift.

There are multiple studies that have described how spectral images can be used to calculate SPRs for proton[50] and heavy-ion treatment.[51] Most techniques use various implementations of the Bethe equation to convert spectral values of each voxel into

SPR,[41,52–55] although stoichiometric calibration can also be applied.[56] Recently, convolutional neural networks have also been proposed to create SPR maps from spectral CT data.[57]

Spectral CT can lower the root mean square errors (RMSE) of proton SPR from 3% to below 1% uncertainty[50] for proton beam therapy, although some articles report clinical errors of 2.2%[58]–2.4%.[59] The reported reasons for this discrepancy are noise and residual beam hardening artifacts, mainly related to the used image-based spectral decomposition technique.[60]

2.4 | Dose calculation in the presence of contrast agent

The use of iodine as a contrast agent is a crucial tool in the visualization of tumors on CT.[61] Iodine has strong attenuation of low KV radiation and thereby increases the HU of perfused areas on CT. This helps with visualization of relevant structures, but it compromises the radiation dose calculation for photon therapy,[62] brachytherapy,[63] and particle therapy.[64] The associated increase of HU generally leads to an overestimation of the attenuation and stopping power, which translates to an underestimation of the dose during photon therapy[62] or a dose range overshoot for particle therapy.[64]

These effects are dependent on the tissue depth and the proximity of organs with strong perfusion, being more prominent in abdominal regions than in areas like the head-and-neck and pelvis. For photon therapy, the uncertainty on dose estimations remains under 1% for most areas, but it can be larger than 2% for abdominal treatment areas.[65] For proton therapy, the effects are more substantial and can result in dose shifts up to 10 mm.[66]

To avoid the influence of iodine contrast on the dose calculations, an additional CT without contrast is typically added to the acquisition protocol for dose calculation. However, this increases imaging dose to the patient and introduces position uncertainty from patient motion between two scans. Therefore, this additional scan is sometimes omitted when dose effects are anticipated to be limited,[67] or the local HU values in regions with high iodine uptake are manually replaced with values of the surrounding tissue.[68]

Spectral CT provides the possibility to create VNC CT scans, with HU similar to conventional CT scans without iodine.[69] Some studies have investigated the use of such scans for the purpose of treatment planning, reporting RMSE deviations of attenuation and stopping powers below 1%, rendering these deviations negligible.[70–72]

For photon therapy, it is also possible to directly produce spectral ED maps for dose planning.[73] Primarily, this would eliminate the need of calibration tables of HU to ED in photon therapy treatment planning. An additional advantage to this approach is that ED measurements are only marginally affected by iodine concentration. A clinically extremely high contrast concentrations of 20 mg/ml iodine is only associated with ED variations of about 5%,[34] while organ perfusion will typically not exceed 2–5 mg/ml, leading to local uncertainties of 1% or less. Using the spectral ED map therefore eliminates significant planning uncertainty that is associated with iodine contrast in conventional CT planning.[74] An illustration of this effect can be seen in Figure 1.

2.5 | Metal artifact reduction

The presence of metal in the body can be a source of major artifacts in CT imaging due to photon starvation, beam-hardening, and scatter effects.[75] Foreign metal objects like hip prostheses,[76] spinal fusion hardware,[77] dental fillings[78] as well as brachytherapy seeds[79] can greatly compromise the calculation of local dose for different RT methods. These artifacts are often handled by manually overwriting affected regions with HU values of normal tissue.[80]

Most contemporary CT scanners provide metal artifact reduction (MAR) algorithms that can reduce these artifacts in conventional CT.[81] MAR algorithms can be applied to conventional data by making assumptions on beam hardening and data that are missing due to photon starvation, and this can improve the accuracy of calculated dose.[82]

The use of spectral CT can also reduce metal artifacts.[76] The reduction of metal artefacts is mainly attributed to the reduction of beam-hardening artefacts in spectral CT.[83] The overall artefact reduction is largest in high KeV VMI, since these have the strongest contribution of the high-energy channel of the DE input data (resulting in minimized photon starvation). MAR algorithms can be combined with spectral high keV VMI to further optimize results.[84]

Reduction of metal artifacts through spectral CT can improve dose calculation for external photon[85–88] and brachytherapy.[89] The impact in dose calculations effects varies largely between metal implant type and size. Although some reported a negligible dose advantage for photon therapy,[90] others reported a reduction of average dose error from 4.4% for conventional CT to 1.1% for a spectral 180 keV.[91]

3 | IMPROVED VISIBILITY LEADS TO INCREASED CERTAINTY

Conventional CT is still the dominant imaging modality in RT for target definition and disease staging,[92] but other imaging modalities are quickly gaining relevancy. Conventional CT is associated with limited soft tissue

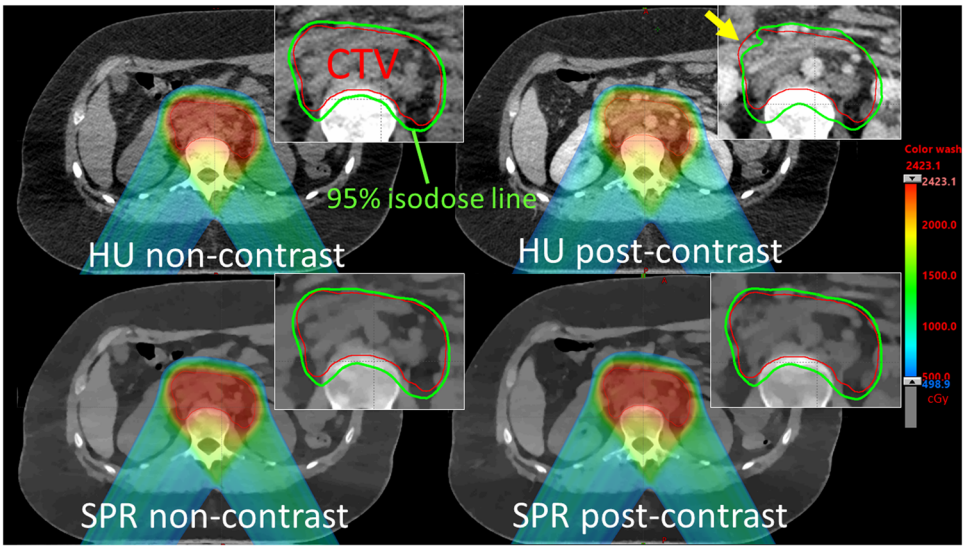

FIGURE 1 Spectral computed tomography (CT) can improve dose calculation in the presence of iodine contrast. This illustration shows comparisons of intensity-modulated proton therapy plans designed on non-contrast images and re-calculated on post-contrast images (Ates 2020). The isodose distributions are nearly identical when spectral stopping power ratio (SPR) images are used for dose calculations. However, the clinical target volume is underdosed when conventional post-contrast conventional Hounsfield unit (HU) images as indicated by the arrow. (Images are courtesy of Dr. Ozgur Ates and Dr. Chiaho Hua from St. Jude Children's Research Hospital, Memphis, TN, USA)

contrast even in the presence of contrast agent and for this other imaging modalities with higher sensitivity and specificity, like positron emission tomography (PET)[93] and magnetic resonance imaging (MRI),[94] are becoming more important in RT.[95]

Spectral CT can improve the contrast of various neoplasms and provides insight on their malignancy.[32] Spectral images generally yield reduced noise[96] and beam hardening artifacts,[6] and by selecting the right spectral results, the visibility of tumors can be optimized.

Low keV VMI maximizes the general iodine contrast in the scan,[27] while high keV VMI data minimize metal artifacts.[30] Z_{eff} can characterize materials based on their chemical composition,[97] and an iodine map visualizes iodine concentrations specifically.[98] These maps improve the visibility of primary tumors, metastases, and involved lymph nodes.

3.1 | Tumor delineation

The use of iodine as an intravenous contrast agent can improve soft tissue contrast on CT. However, the increase of perfusion can often be very subtle (e.g., prostate tumors, see Figure 2[99]) or even hypodense in comparison to the surrounding parenchyma (e.g., pancreatic adenocarcinoma[100]). This lack of contrast can cause stark variations in target delineations of many treatment areas[101] for head and neck,[102] gastric,[103] pancreatic,[104] prostate,[105] bladder,[106] and even pulmonary[107] cancers.

Various radiological studies have proven that spectral CT improves tumor visibility, by improving the tumor contrast for malignancies such as lymphomas,[108] head and neck (H&N) lesions,[109–112] lung cancer,[113] breast,[114] pancreatic cancer,[115–117] prostate cancer,[118] gynaecological cancer,[119] urothelial carcinoma,[120] and hepatocellular carcinoma (HCC).[121] All studies indicate that low keV VMI images yield increased contrast-to-noise (CNR) of the tumor in comparison to conventional CT. The increase of CNR was very dependent of tumor type as well as acquisition and reconstruction methods, ranging from 36.6% for H&N cancer[109] to 62.3% for bladder cancer.[120] Tumors located near metal implants are an exception, since high VMI images yield minimalization of metal artifacts.[122,123]

Two articles compared tumor PET uptake to iodine contrasts of the tumor on spectral CT. One study compared the ability of spectral CT to predict microscopic invasiveness for non-small cell lung cancers (NSCLCs) to that of ^{18}F-Fluorodeoxyglucose (FDG) PET, finding that the diagnostic performance of both modalities was similar.[124] Another study found high correlation (R^2=0.82) between PET standard uptake values (SUVs) and multiple spectral CT features in patients with pancreatic adenocarcinoma, concluding that spectral CT is a potential surrogate for FDG in assessment of these tumors.[125]

Although a lot of articles claim to have investigated the impact of spectral CT on tumor delineation, most have merely investigated features like SNR and CNR. Only one study really reported the effect of image quality improvement on delineation variability. A comparison of spectral CT with MRI finds that 60 keV VMI provided a higher interobserver agreement for non-skull base tumors in comparison to T1 with contrast and T2

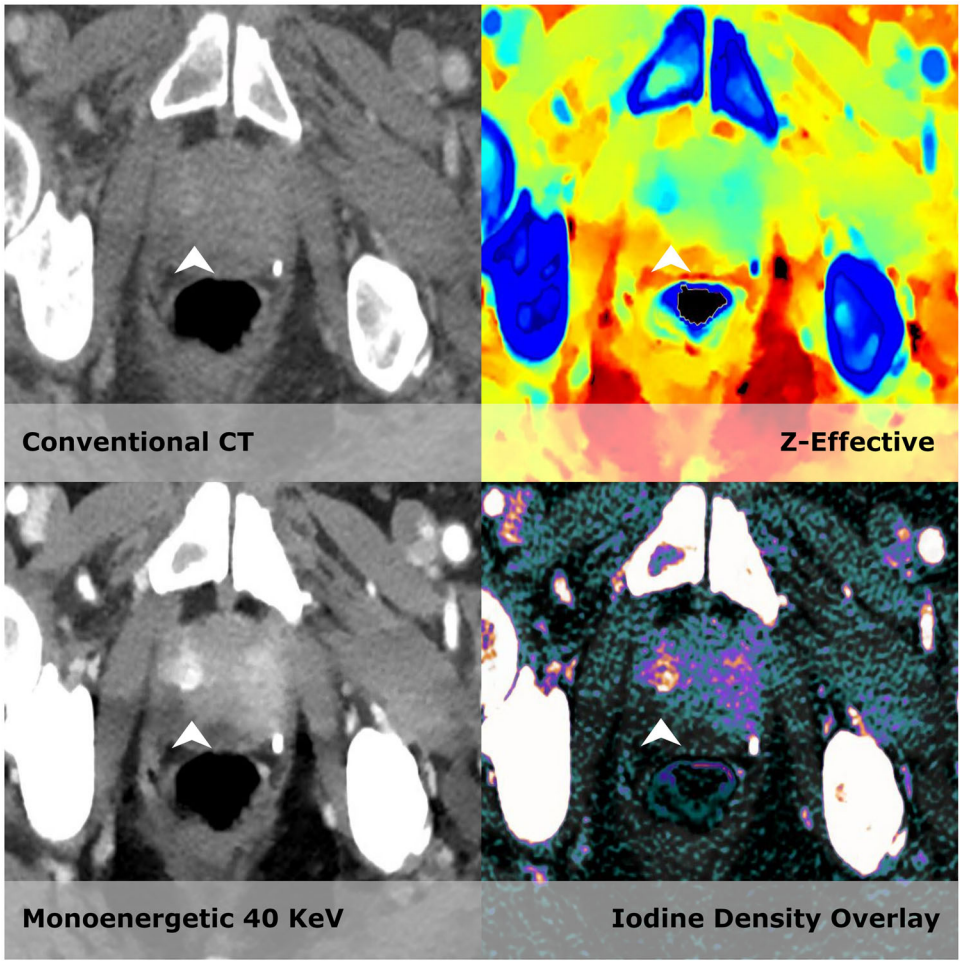

FIGURE 2 Computed tomography (CT)-based radiotherapy (RT) treatment of the prostate often aims for the entire gland, because the tumor is usually hardly visible on conventional CT. Magnetic resonance imaging (MRI) data are therefore commonly added to define the exact tumor extent within the gland. This figure is an example of an 82-year-old male with biopsy-proven prostate cancer (Gleason 3 + 4 = 7) in the right side of the gland (arrow), demonstrating that spectral CT allows for better discrimination of the tumor. It is very likely that this information can be used to improve treatment precision. (Images are courtesy of Dr. Michael Brun Andersen and prof. Dr. Finn Rasmussen from Aarhus University Hospital)

weighted MRI.[126] A limitation to this study is that the results are not compared to conventional CT, making it impossible to attribute the specific benefits of spectral CT over conventional CT.

3.2 | Staging of lymph nodes and metastasis

Improved contrast not only increases the visibility of the main tumor, also metastasis and lymph nodes become more apparent, which is crucial for disease staging. Although staging is not typically performed in RT departments, it is still helpful to detect and assess the malignancy of lymph nodes and metastasis at the time of RT planning.

For the detection of metastasis, many of the relevant techniques are similar to the detection and delineation of the main tumor. However, for correct assessment of hyperdense findings, it is essential to discriminate iodine from other contrasts to determine malignancy.[32] Spectral CT can be very useful for the detection and assessment of lung,[127] liver,[128] bone,[129] brain,[130] and adrenal metastasis,[131] as well as local invasion of gastric[132] and lung cancer.[133]

This is also the case for determination of lymph node involvement. For assessment of the lymph node stations, assessment of node size is not enough; it is crucial to assess texture, local perfusion, and the pattern of perfusion within the nodes.[134–136] By visualization and quantification of iodine,[137] spectral images help in the assessment the malignancy of lymph nodes in the abdomen,[138] HCC,[139] H&N,[140–142] gastric[143,59], pulmonary,[168] colorectal,[144] and rectal cancer.[145,146]

Within RT, PET, and MRI currently play an integral role in RT staging of many cancer types. To our knowledge,

there is no literature on direct comparisons between the performance of these modalities to spectral CT on staging. There are, however, two studies that demonstrate the additional value of spectral CT to PET in staging of single osteolytic metastases of resectable NSCLC[147] and to both MRI and PET for staging of H&N cancer.[148]

3.3 | Organs-at-risk delineation

Delineation of OAR is crucial for sparing of these organs, but especially in areas with complex anatomy like the head and neck, discrimination of different organs-at-risk can be challenging on conventional CT.[149] But even in simpler anatomies, improved organ discrimination might help with automation of the delineation process.[150]

Spectral CT increases HU stability,[151] and the concept of spectral fingerprinting[152] might raise the possibility to describe tissue types, based on specific CT features, which would aid tissue segmentation for the purpose of OAR definition. A number of studies report that spectral CT improves the performance of artificial intelligence (AI) for the purpose of auto-delineation for various abdominal organs,[153] bones[154] as well as OARs in the head.[155,156]

4 | QUANTIFICATION LEADS TO PATIENTS-SPECIFIC CARE

CT is by nature a scanning technique that provides anatomical information. The introduction of a contrast agent to a conventional CT scan can add quantitative information on physiologic features like perfusion and ventilation. But in order to quantify local concentrations, a dynamic scan is necessary, complicating the acquisition protocol at an elevated dose.

Spectral material decomposition allows for quantification of local contrast agent concentrations in a single static scan, which potentially could be used as a replacement for dynamic scans for tumor differentiation, treatment response analyses, adaptive treatments, and elective strategies to save functional parts of organs-at-risk.

4.1 | Tumor differentiation

Traditionally, RT aims to administer a homogeneous dose to the delineated tumor. However, it is known that hypoxia, proliferation, and other functional factors have a local influence on radiation sensitivity of cancers.[157] Therefore, inhomogeneous dose can be prescribed by either giving a boost within a delineated tumor[158,91] or by abandoning delineation and use a concept of tumor probability[159] or dose-painting-by-numbers[160] for local dose prescription based on functional imaging.

PET and MRI are primarily used for assessing local tumor physiology. The role of conventional CT has been limited in functional tumor differentiation, because static CT provides little functional information. There have been attempts to use dynamic contrast enhanced (DCE) CT[161] for various RT applications, but due to increased imaging dose, limited scan FOV and general scan complexity associated with DCE CT, DCE MRI is generally favored instead.[162] The use of local perfusion parameters from DCE CT or MRI has been described extensively for target definition in diseases like prostate cancer[163] and pulmonary cancers.[164]

Spectral CT allows quantification of local tumor perfusion from a static contrast enhanced CT, by quantification of the iodine concentrations at one timepoint (see Figure 3). Although this technique does not provide elaborate DCE features like vascular permeability and mean transit time, it is regarded as an indicator of local perfusion.[165]

For lung tumors, spectral iodine quantification values have been demonstrated to be associated with tumor differentiation[166] and proliferation.[167–169] Another study describes the use of normalized iodine concentration as a biomarker for the aggressiveness of rectal cancer.[170] Potentially this information could be used for dose description, although to our knowledge, there is no study that describes this application.

It is, however, important to realize that timing of the scan is crucial. There are several studies that assess the correlation of FDG PET uptake to spectral CT iodine maps in lung cancer. One study found a positive correlation between the maximum SUV (SUV_{max}) and the maximum iodine concentration ($Iodine_{max}$) in late arterial phase,[171] while another study finds a negative relationship between SUV_{max} and iodine concentrations in the venous phase.[172]

In a recent study, it was demonstrated that also distribution patterns can provide prognostic value for recurrence after SBRT of lung cancer.[173] It was reported that the ratio between the low-density area and the total tumor volume was negatively predictive for outcome, illustrating that heterogeneity of perfusion in the tumor might be relevant to the treatment plan.

4.2 | Treatment response monitoring

Changes in tumor and normal tissue perfusion, during and after therapy, can be an indicator of treatment efficacy as well as damage inflicted to the surrounding parenchyma. For this reason, DCE MRI and CT are often used to monitor treatment effects of various treatment modalities on different cancer types.[174–176]

There have been a number of articles that describe that perfusion parameters can be used for treatment response of RT, specifically for various tumor types, like

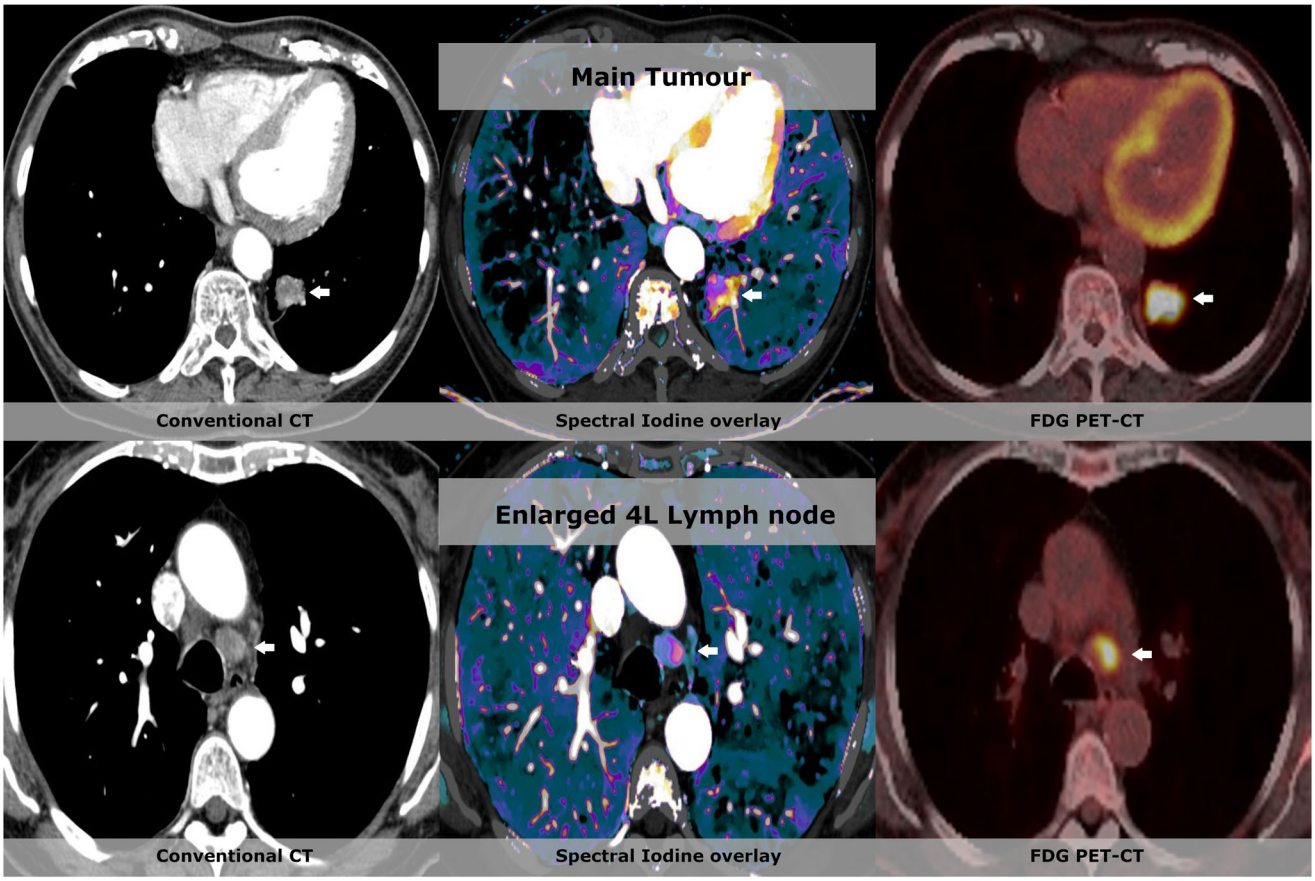

FIGURE 3 Spectral iodine quantification can be used to differentiate within the tumor and lymph nodes. This figure shows data from a 75-year-old male with lung cancer. In the top row, the conventional series show a 25 mm tumor paravertebral in the left lower lobe with slight enhancement. The iodine map shows that there is iodine uptake in the entire tumor with strong increased perfusion in the lateral and posterior part of the tumor, where corresponding positron emission tomography (PET) images show 8F-Fluorodeoxyglucose (FDG) uptake in the entire tumor. The patient also had an enlarged 4L lymph node of 14 mm in short axis. The corresponding iodine overlay shows a similar perfusion and FDG uptake pattern in the left side of the lymph node. (Images are courtesy of Dr. Michael Brun Andersen and prof. Dr. Finn Rasmussen from Aarhus University Hospital)

rectal,[177–179] pulmonary,[180,181] cervical,[182–184] H&N,[185] and pancreatic cancers.[186]

Since spectral iodine maps are an indicator of local perfusion, they have been used to monitor targeted therapies for diseases like gastrointestinal stromal tumors[187,188] and NSCLC.[189] More recently studies have demonstrated the feasibility of monitoring RT outcomes with spectral CT for lung,[190] cervical,[191] pancreatic,[192] and H&N cancers.[193,194]

In two studies, iodine quantification through spectral CT to assess treatment response of lung cancers to chemoradiotherapy and RT was compared to FDG PET. It was found that both modalities correlated well, indicating the feasibility for substitution of the PET follow-up scan with a spectral CT exam.[195,196]

Also, for rectal cancers spectral iodine quantification can be used for response evaluation. In a study from 2020, Sauter at al.[197] demonstrated a very strong correlation ($r = 0.73$; $p = 0.01$) between the changes of both spectral iodine quantification and MRI-based mean apparent diffusion coefficient (ADC), in follow-up scans of patients that underwent radiochemotherapy. Since ADC MRI is considered the gold standard for response evaluation in rectal cancer and because of the strong correlation, they concluded that spectral iodine quantification could be a good alternative.

Another study investigated the potential use of spectral iodine maps for follow-up imaging of NSCLC after chemoradiotherapy.[198] In this study, a correlation was found between local iodine values in the tumor and disease progression as defined by RECIST criteria. Patients with disease progression also demonstrated higher iodine hotspots directly after treatment, indicating remaining vital tumor tissue.

4.3 | Functional sparing of organs-at-risk

Functional discrimination within OARs might raise the possibility to spare healthy parts of OARs, over

less-functioning parts. Some studies have used ventilation[199] and perfusion[79] parameters to selectively spare healthy lung tissues.

The imaging standard for assessment of pulmonary function in diseases like chronic obstructive pulmonary disease is combined ventilation/perfusion single-photon emission CT (SPECT). This technique, however, lacks high spatial resolution[200] and general availability in RT clinics. For this reason, assessment of perfusion through other modalities, like PET and CT, is favorable, and it has been demonstrated that spectral iodine maps can be used as a replacement of perfusion SPECT, for the sparing of functional lung tissue.[201]

Some groups have also attempted to assess lung ventilation through conventional CT techniques like 4D CT[202] and dynamic imaging with krypton or xenon gas as a contrast agent.[203] Xenon quantification can be performed by conventional subtraction CT,[204] but visualization and quantification are generally improved by spectral CT,[205] even for dynamic scans[206]). By combining these data with spectral iodine perfusion scans, a ventilation/perfusion CT can be constructed.[207,208]

Since iodine and xenon have similar attenuating features, it is not possible to discriminate them on a single spectral CT. However, by replacing iodine with gadolinium as an intravenous contrast agent, it has been demonstrated that it is feasible to acquire a ventilation/perfusion CT with one spectral scan through three-material differentiation.[209]

The potential of sparing functional tissue is not limited to pulmonary treatments only. In a recent study, spectral iodine maps were used to minimize the dose to the functional parts of the liver.[210] It was demonstrated that this was possible, without compromising target coverage.

5 | DISCUSSION

Spectral CT is becoming an established technique in radiology. There is extensive and convincing proof that spectral CT adds relevant radiological information for various tumors.[32,211–213]

The main application of spectral CT in RT is for the creation of SPR to improve dose calculation in proton therapy. However, by improving tumor contrast and adding functional information, spectral CT could potentially pose an alternative for PET and MRI, hereby reducing treatment cost and complexity. But although it is tempting to extrapolate this radiological value toward the RT clinic, there is a need to test this hypothesis in clinical studies in an RT setting.[211]

Although PC CT systems are not yet clinically available, and RT applications have not been tested, the values that are described in this article will likely apply to this technique as well. Especially with regard to tumor quantification and visualization, PC CT has large potentials, due to the ability to potentially use new contrast agents and better quantify tissue composition.[28] For dose calculation, the improved quantification of tissue make-up could improve for instance Monte Carlo simulation.

Recent usability improvements of spectral CT have facilitated clinical adoption,[214] but it still needs to establish its position in radiation oncology.[33] It has been critical for radiologic adoption of spectral CT that the technique does not negatively impact workflow and patient throughput.[214]

Sequential DE-CT protocols are available on most contemporary CT simulators and are being used in RT for applications like SPR calculations,[19] contrast enhancement,[156] and 4D CT imaging.[12] They might remain an alternative to the much more expensive integrated spectral solutions, in spite of their limitations in applications, quantitative features, and data integration.

An alternative approach would be to register an extra diagnostic spectral CT scan to the conventional planning CT, but this would complicate the workflow and render the conventional planning CT largely redundant. The use of a spectral CT scanner from a radiology department as a simulator could pose as a solution, but this could result in patient/staff scheduling complexity, since it would require interdepartmental cooperation. The scanners could furthermore compromise on specific RT needs, like bore size.

The optimal implementation option seems to be an integrated spectral solution, which is lacking in the current generation of CT scanners dedicated for RT simulation. An integrated spectral CT simulator would require significant design modifications, which can only be justified by considerable benefits for the majority of RT use cases. Spectral CT is currently mainly used in institutions that offer particle therapy for the promise of improved treatment planning, but it needs to demonstrate a broader benefit to exert a stronger impact on the radiation oncology community.

The increased disease visibility and quantifiability that are associated with spectral CT are potentially beneficial for all treatment modalities and might even be crucial for the future of CT simulation. However, most of these potentials require iodine as a contrast agent, which is problematic for sequential DE-CT due to limitations in temporal resolution. The lack of an integrated spectral RT solution is therefore part of the reason that the application of spectral CT in RT is limited to applications that do not require high temporal resolution, like dose planning for particle therapy.[50]

Over the past two decades, the need for functional imaging in RT has increased both for staging,[215] treatment planning,[95] and response assessment.[92] As a result, the demand for[216,93] and access to[217] both PET and MRI in RT departments has increased significantly over the last two decades, thereby potentially reducing the role for CT to mere dose calculation and cone-beam

position verification.[218] The integration of MR scanners during RT treatment,[219] as well as the development of MR-based synthetic CT images[220,221] enable an MR-only workflow,[222] which could potentially erode the value of CT in RT.[223]

Although both PET and MRI provide useful information, both bring limitations to a nimble RT clinic. Both modalities are expensive, complex, time-consuming and require specialized staff that needs to be trained in the RT department or lend from other department to safely operate the scanners.[206,224,225] MRI is associated with reduced geometric fidelity, and PET is associated with low intrinsic resolution. PET also requires expensive, short-lived radioactive tracers and requires long preparation procedures of fasting and resting prior to the scan, which hamper integration into adaptive RT schemes.[226] Furthermore, both PET and MRI have typical acquisition times in the order of 15–60 min, which limit throughput and pose a challenge for dynamic organs. In comparison to that, CT is much faster with acquisitions in the order of singular minutes.

Another issue for both MRI and PET is reproducibility. To be able to use quantitative results for local dose prescription, reproducibility of results between patients and vendors is paramount. Both PET[227] and MRI[216,95] have a vast number of acquisition parameters that can influence measurements. There are many efforts to homogenize outcomes, but it remains challenging to assure reproducibility between patients and machines. This is problematic when local values are directly linked to local dose definition.[160]

CT results are much more reproducible, because the interaction of radiation with tissues is well defined.[36] Spectral CT adds precision to conventional CT since it largely eliminates the effects of tube output and beam hardening on the results (in the case of sinogram-based decomposition).[10] This makes the results more reproducible and very suitable for direct dose prescription, although small differences between implementations of vendors exist.[228]

Spectral CT constitutes a wide variety of results, but how to practically implement these results into the RT clinic remains to be investigated. Because of the quantitative values of spectral CT results, spectral SPR or ED results could theoretically be sent straight to the treatment planning system to replace the planning CT, eliminating the need for a lookup table. But to incorporate different keV images, iodine and Z-effective maps into the delineation process would require careful considerations to maximize efficiency and avoid incorrect use of images that jeopardize patient safety. It is likely that we could learn much from how different parametric images of PET and MRI results were introduced into treatment planning.

The development of AI could aid implementation of spectral CT. The performance of AI benefits from an increased number of parameters,[229,230] and the use of spectral CT will therefore likely improve the outcome of such algorithms. AI could help to manage large amounts of data, by aiding the radiation oncologist in their analyses. AI has already been applied to spectral CT data to detect lesions,[231] predefine OARs,[155] and assess involved lymph nodes.[232] It is therefore likely that spectral CT and AI will develop in a symbiotic manner, where spectral CT improves the performance of different tasks performed by AI, while AI could make the associated data-load manageable.

ACKNOWLEDGMENTS

The author would like to thank the reviewers of this journal, Dr. Chia-Ho Hua from St. Jude's Children's Research Hospital in Memphis (USA), Dr. Jeroen van de Kamer from the Netherlands Cancer Institute in Amsterdam (the Netherland), Dr. Michael Brun Andersen from Copenhagen University Hospital (Denmark), prof. Dr. Finn Rasmussen from Aarhus University Hospital (Denmark) and Scott Smith, Dr. Yoad Yagil, Dr. Lizette Warner, and Walter Giepmans, from Philips, for their critical feedback, discussions, proofreading, and contributions to this review. Special thanks are extended to Dr. Ozgur Ates, Dr. Chia-Ho Hua, Dr. Michael Brun Andersen and prof. Dr. Finn Rasmussen for their help in providing the Figures in this article.

CONFLICT OF INTEREST

The author is an employee of Philips Healthcare.

DATA AVAILABILITY STATEMENT

Data sharing is not applicable to this article as no datasets were generated or analyzed during the current study.

REFERENCES

1. Jane Dobbs H, Parker RP, Hodson NJ, Hobday P, Husband JE The use of CT in radiotherapy treatment planning. *Radiother Oncol*. 1983;1(2):133-141. https://doi.org/10.1016/S0167-8140(83)80016-4.
2. Kijewski PK, Bjarngard BE. Correction for beam hardening in computer tomography. *Med Phys*. 1978;5:209-214.
3. Neitzel U, Kosanetzky J, Harding G. Coherent scatter in radiographic imaging: a Monte Carlo simulation study. *Phys Med Biol*. 1985;30(12):1289-1296. https://doi.org/10.1088/0031-9155/30/12/002.
4. Alvarez RE, Macovski A. Energy-selective reconstructions in X-ray computerized tomography. *Physics in Medicine and Biology*, 1976;21(5):733-744. https://doi.org/10.1088/0031-9155/21/5/002
5. Yu L, Leng S, McCollough CH. Dual-energy CT-based monochromatic imaging. *Am J Roentg*. 2012;199(5):9-15. https://doi.org/10.2214/AJR.12.9121.
6. Maaß C, Baer M, Kachelrieß M. Image-Based Dual Energy CT Using Optimized Precorrection Functions: A Practical New Approach to Material Decomposition in the Image Domain. Springer; 2009. https://doi.org/10.1007/978-3-642-03879-2-58.
7. Parakh A An C, Lennartz S, et al. Recognizing and minimizing artifacts at dual-energy CT. *Radiographics*. 2021;41(2):509-523.
8. Zhang S, Han D, Politte DG, Williamson JF, O'Sullivan JA. Impact of joint statistical dual-energy CT reconstruction of proton stopping power images: comparison to image- and

sinogram-domain material decomposition approaches. *Med Phys.* 2018;45(5):2129-2142. https://doi.org/10.1002/mp.12875.
9. Hounsfield G. Computerized transverse axial scanning (tomography): part I. Description of system. *Br J Radiol.* 1973;46:1016–1022. https://doi.org/10.1016/0360-3016(94)E0127-6.
10. McCollough CH, Boedeker K, Cody D, et al. Principles and applications of multi-energy CT: report of AAPM task group. *Med Phys.* 2020:47:e881-e912. https://doi.org/10.1002/mp.14157.
11. Forghani R, De Man B, Gupta R. Dual-energy computed tomography physical principles, approaches to scanning, usage, and implementation: part 1. *Neuroimaging Clin N Am*. 2017;27(3):385-400. https://doi.org/10.1016/j.nic.2017.03.003.
12. Wohlfahrt P, Troost EGCC, Hofmann C, Richter C, Jakobi A. Clinical feasibility of single-source dual-spiral 4D dual-energy CT for proton treatment planning within the thoracic region. *Int J Radiat Oncol Biol Phys.* 2018;102(4):830-840. https://doi.org/10.1016/j.ijrobp.2018.06.044.
13. Euler A, Falkowski AL, Parakh A, Falkowski AL. Initial results of a single-source dual-energy computed tomography technique using a split-filter: assessment of image quality, radiation dose, and accuracy of dual-energy applications in an in vitro and in vivo study. *Invest Radiol*. 2016;51(8):491-498. https://doi.org/10.1097/RLI.0000000000000257.
14. Almeida IP, Schyns LEJR, Ollers MC, et al. Dual-energy CT quantitative imaging: a comparison study between twin-beam and dual-source CT scanners. *Med Phys.* 2017;44(1):171-179. https://doi.org/10.1002/mp.12000.
15. Pérez-Lara A, Forghani R. Spectral computed tomography: technique and applications for head and neck cancer. *Magn Reson Imaging Clin N Am.* 2018;26:1-17.
16. Graser A, Johnson TRC, Bader M, et al. Dual energy CT characterization of urinary calculi: initial in vitro and clinical experience. *Invest Radiol.* 2008;43:112-119.
17. Choi HK, Al-Arfaj AM, Eftekhari A, et al. Dual energy computed tomography in tophaceous gout. *Ann Rheum Dis.* 2009;68:1609-1612.
18. Mendler MH, Bouillet P, Sidaner ALe, et al. Dual-energy CT in the diagnosis and quantification of fatty liver: limited clinical value in comparison to ultrasound scan and single-energy CT, with special reference to iron overload. *J Hepatol.* 1998;28(5):785-794. https://doi.org/10.1016/S0168-8278(98)80228-6.
19. Wohlfahrt P, Möhler C, Hietschold V, et al. Clinical implementation of dual-energy CT for proton treatment planning on pseudo-monoenergetic CT scans. *Int J Radiat Oncol Biol Phys.* 2017;97:427-434.
20. Zhu J, Penfold SN. Dosimetric comparison of stopping power calibration with dual energy CT and single energy CT in proton therapy treatment planning. *Med Phys.* 2016;43(6):2845-2854.
21. Megibow AJ, Kambadakone A, Ananthakrishnan L. Dual-energy computed tomography: image acquisition, processing, and workflow. *Radiol Clin North Am.* 2018;56(4):507-520. https://doi.org/10.1016/j.rcl.2018.03.001.
22. Flohr TG, Mccollough CH, Sü C, Primak AN, Ohnesorge BM. First performance evaluation of a dual-source CT (DSCT) system. *Eur Radiol*. 2006;16:256-268. https://doi.org/10.1007/s00330-005-2919-2.
23. Chandra N, Langan DA. Gemstone detector: dual energy imaging via fast kVp switching. In: Johnson T, Fink C, Schönberg S, Reiser M, eds. Dual Energy CT in Clinical Practice. Medical Radiology. Springer; 2011. https://doi.org/10.1007/174_2010_35.
24. McCollough CH, Leng S, Yu L, Fletcher JG. Dual-and multi-energy CT: principles, technical approaches, and clinical applications. *Radiology*. 2015;276(3):637-653. https://doi.org/10.1148/radiol.2015142631.
25. Vlassenbroek A. Dual layer CT. In: Johnson T, Fink C, Schönberg S, Reiser M, eds. *Dual Energy CT in Clinical Practice*. *Medical Radiology*. Springer; 2011. https://doi.org/10.1007/174_2010_56.
26. Fredenberg E. Spectral and dual-energy X-ray imaging for medical applications. *Nucl Instruments Methods Phys Res Sect A Accel Spectrometers Detect Assoc Equip.* 2018;878:74-87.
27. Sellerer T, Noël PB, Patino M, et al. Dual-energy CT : a phantom comparison of different platforms for abdominal imaging. *Eur Radiol.* 2018;28:2745–2755. https://doi.org/10.1007/s00330-017-5238-5.
28. Flohr T, Petersilka M, Henning A, Ulzheimer S, Ferda J, Schmidt B. Photon-counting CT review. *Physica Med.* 2020;79:126-136.
29. Große Hokamp N, Gilkeson R, Jordan MK, et al. Virtual monoenergetic images from spectral detector CT as a surrogate for conventional CT images: unaltered attenuation characteristics with reduced image noise. *Eur J Radiol.* 2019;117:49-55.
30. Bamberg F, Dierks A, Nikolaou K, Reiser MF, Becker CR, Johnson TRC. Metal artifact reduction by dual energy computed tomography using monoenergetic extrapolation. *Eur Radiol.* 2011;21(7):1424-1429. https://doi.org/10.1007/s00330-011-2062-1.
31. Soesbe TC, Ananthakrishnan L, Lewis MA, et al. Pseudoenhancement effects on iodine quantification from dual-energy spectral CT systems: a multi-vendor phantom study regarding renal lesion characterization. *Eur J Radiol.* 2018;105(11):125-133. https://doi.org/10.1016/j.ejrad.2018.06.002.
32. Andersen MB, Ebbesen D, Thygesen J, Kruis M, Rasmussen F. Impact of spectral body imaging in patients suspected for occult cancer : a prospective study of 503 patients. *Eur Radiol* 2020;30(10):5539-5550.
33. Van Elmpt W, Landry G, Das M, Verhaegen F. Dual energy CT in radiotherapy: current applications and future outlook. *Radiother Oncol.* 2016;119(1):137-144. https://doi.org/10.1016/j.radonc.2016.02.026.
34. Hua CH, Shapira N, Merchant TE, et al. Accuracy of electron density, effective atomic number, and iodine concentration determination with a dual-layer dual-energy computed tomography system. *Med Phys*. 2018;45(6):2486-2497. https://doi.org/10.1002/mp.12903.
35. Swindell W. A 4MV CT scanner for radiation therapy; spectral properties of the therapy beam. *Med Phys.* 1983;10(3):347-351. https://doi.org/10.1118/1.595280.
36. Phelps ME, Gado MH, Hoffman EJ. Correlation of effective atomic number and electron density with attenuation coefficients measured with polychromatic X rays. *Radiology*. 1975;117(3 I):585-588. https://doi.org/10.1148/117.3.585.
37. Thomas SJ. Relative electron density calibration of CT scanners for radiotherapy treatment planning. *Br J Radiol.* 1999;72(7):781-786. https://doi.org/10.1259/bjr.72.860.10624344.
38. Devic S, Monroe JI, Mutic S, Whiting B, Williamson JF. Dual energy CT tissue quantitation for Monte-Carlo based treatment planning for brachytherapy. Paper presented at: Annual International Conference of the IEEE Engineering in Medicine and Biology - Proceedings; July 23-28, 2000; Chicago, IL. https://doi.org/10.1109/IEMBS.2000.900750.
39. Knopf A-C, Lomax A. In vivo proton range verification: a review. *Phys Med Biol Phys Med Biol.* 2013;58(58):131-160. https://doi.org/10.1088/0031-9155/58/15/R131.
40. Landry G, Reniers B, Murrer L, et al. Sensitivity of low energy brachytherapy Monte Carlo dose calculations to uncertainties in human tissue composition. *Med Phys.* 2010;37(10):5188-5198. https://doi.org/10.1118/1.3477161.
41. Lalonde A, Bouchard H. A general method to derive tissue parameters for Monte Carlo dose calculation with multi-energy CT. *Phys Med Biol.* 2016;61(22):8044-8069. https://doi.org/10.1088/0031-9155/61/22/8044.
42. Schneider W, Bortfeld T, Schlegel W. Correlation between CT numbers and tissue parameters needed for Monte Carlo simulations of clinical dose distributions. *Phys Med Biol.* 2000;45(2):459-478. https://doi.org/10.1088/0031-9155/45/2/314.

43. Verhaegen F, Devic S. Sensitivity study for CT image use in Monte Carlo treatment planning. *Phys Med Biol.* 2005;50(5):937-946. https://doi.org/10.1088/0031-9155/50/5/016.
44. Landry G, Granton PV, Reniers B, et al. Simulation study on potential accuracy gains from dual energy CT tissue segmentation for low-energy brachytherapy Monte Carlo dose calculations. *Phys Med Biol.* 2011;56(19):6257-6278. https://doi.org/10.1088/0031-9155/56/19/007.
45. Hünemohr N, Paganetti H, Greilich S, Jäkel O, Seco J. Tissue decomposition from dual energy CT data for MC based dose calculation in particle therapy. *Med Phys.* 2014;41(6):1-14. https://doi.org/10.1118/1.4875976.
46. Han D, Porras-Chaverri MA, O'Sullivan JA, Politte DG, Williamson JF. Technical note: on the accuracy of parametric two-parameter photon cross-section models in dual-energy CT applications. *Med Phys.* 2017;44:2438-2446.
47. Malusek A, Karlsson M, Magnusson M, Carlsson GA. The potential of dual-energy computed tomography for quantitative decomposition of soft tissues to water, protein and lipid in brachytherapy. *Phys Med Biol.* 2013;58(4):771-785. https://doi.org/10.1088/0031-9155/58/4/771.
48. Williamson JF, Li S, Devic S, Whiting BR, Lerma FA. On two-parameter models of photon cross sections: application to dual-energy CT imaging. *Med Phys.* 2006;33(11):4115-4129. https://doi.org/10.1118/1.2349688.
49. Remy C, Lalonde A, Béliveau-Nadeau D, Carrier JF, Bouchard H. Dosimetric impact of dual-energy CT tissue segmentation for low-energy prostate brachytherapy: a Monte Carlo study. *Phys Med Biol.* 2018;63:025013.
50. Wohlfahrt P, Richter C. Status and innovations in pre-treatment CT imaging for proton therapy. *Br J Radiol.* 2020;93(1107):20190590.
51. Faller FK, Mein S, Ackermann B, Debus JJJ, Stiller W, Mairani A. Pre-clinical evaluation of dual-layer spectral computed tomography-based stopping power prediction for particle therapy planning at the Heidelberg Ion Beam Therapy Center. *Phys Med Biol.* 2020;65(9):095007. https://doi.org/10.1088/1361-6560/ab735e.
52. Saito M, Sagara S. Simplified derivation of stopping power ratio in the human body from dual-energy CT data. *Med Phys*. 2017;44(8):4179-4187. https://doi.org/10.1002/mp.12386.
53. Yang M, Virshup G, Clayton J, Zhu XR, Mohan R, Dong L. Theoretical variance analysis of single- and dual-energy computed tomography methods for calculating proton stopping power ratios of biological tissues. *Phys Med Biol.* 2010;55(5):1343-1362. https://doi.org/10.1088/0031-9155/55/5/006.
54. Almeida IP, Schyns LEJR, Vaniqui A, et al. Monte Carlo proton dose calculations using a radiotherapy specific dual-energy CT scanner for tissue segmentation and range assessment. *Phys Med Biol.* 2018;63(11):115008. https://doi.org/10.1088/1361-6560/aabb60.
55. Han D, Siebers JV, Williamson JF. A linear, separable two-parameter model for dual energy CT imaging of proton stopping power computation. *Med Phys.* 2016;43(1):600-612. https://doi.org/10.1118/1.4939082.
56. Bourque AE, Carrier JF, Bouchard H. A stoichiometric calibration method for dual energy computed tomography. *Phys Med Biol*. 2014;59(8):2059-2088. https://doi.org/10.1088/0031-9155/59/8/2059.
57. Lee HHC, Park YK, Duan X, Jia X, Jiang S, Yang M. Convolutional neural network based proton stopping-power-ratio estimation with dual-energy CT: a feasibility study. *Phys Med Biol*. 2020;65:215016.
58. Li B, Lee HC, Duan X, et al. Comprehensive analysis of proton range uncertainties related to stopping-power-ratio estimation using dual-energy CT imaging. *Phys Med Biol.* 2017;62:7056-7074.
59. Bär E, Lalonde A, Royle G, et al. The potential of dual-energy CT to reduce proton beam range uncertainties. *Med Phys*. 2017;44(6):2332-2344. https://doi.org/10.1002/mp.12215.
60. Li J, Fang M, Wang R, et al. Diagnostic accuracy of dual-energy CT-based nomograms to predict lymph node metastasis in gastric cancer. *Eur Radiol.* 2018;28:5241-5249.
61. Rutten A, Prokop M. Contrast agents in X-ray computed tomography and its applications in oncology. *Anticancer Agents Med Chem.* 2007;7:307-316.
62. Ramm U, Damrau M, Mose S, Manegold KH, Rahl CG, Böttcher HD. Influence of CT contrast agents on dose calculations in a 3D treatment planning system. *Phys Med Biol*. 2001;46(10):2631-2635. https://doi.org/10.1088/0031-9155/46/10/308.
63. Li XA. Dosimetric effects of contrast media for catheter-based intravascular brachytherapy. *Med Phys*. 2001;28(5):757-763. https://doi.org/10.1118/1.1367279.
64. Wertz H, Jäkel O. Influence of iodine contrast agent on the range of ion beams for radiotherapy. *Med Phys.* 2004;31(4):767-773. https://doi.org/10.1118/1.1650871.
65. Shibamoto Y, Naruse A, Fukuma H, Ayakawa S, Sugie C, Tomita N. Influence of contrast materials on dose calculation in radiotherapy planning using computed tomography for tumors at various anatomical regions: a prospective study. *Radiother Oncol.* 2007;84(1):52-55. https://doi.org/10.1016/j.radonc.2007.05.015.
66. Hwang UJ, Shin DH, Kim TH, et al. The effect of a contrast agent on proton beam range in radiotherapy planning using computed tomography for patients with locoregionally advanced lung cancer. *Int J Radiat Oncol Biol Phys.* 2011;81(4):E317-E324. https://doi.org/10.1016/j.ijrobp.2011.02.025.
67. Létourneau D, Finlay M, O'Sullivan B, et al. Lack of influence of intravenous contrast on head and neck IMRT dose distributions. *Acta Oncol (Madr).* 2008;47(1):90-94. https://doi.org/10.1080/02841860701418861.
68. Stern RL, Heaton R, Fraser MW, et al. Verification of monitor unit calculations for non-IMRT clinical radiotherapy: Report of AAPM Task Group 114. *Med Phys.* 2011;38:504-530.
69. Sauter AP, Muenzel D, Dangelmaier J, et al. Dual-layer spectral computed tomography: virtual non-contrast in comparison to true non-contrast images. *Eur J Radiol.* 2018;104(11):108-114. https://doi.org/10.1016/j.ejrad.2018.05.007.
70. Yamada S, Ueguchi T, Ogata T, et al. Radiotherapy treatment planning with contrast-enhanced computed tomography: feasibility of dual-energy virtual unenhanced imaging for improved dose calculations. *Radiat Oncol.* 2014;9(1):168. https://doi.org/10.1186/1748-717X-9-168.
71. Lalonde A, Xie Y, Burgdorf B, et al. Influence of intravenous contrast agent on dose calculation in proton therapy using dual energy CT. *Phys Med Biol.* 2019;64:125024.
72. Lapointe A, Lalonde A, Bahig H, Carrier JF, Bedwani S, Bouchard H. Robust quantitative contrast-enhanced dual-energy CT for radiotherapy applications. *Med Phys*. 2018;45(7):3086-3096. https://doi.org/10.1002/mp.12934.
73. Mohler C, Wohlfahrt P, Richter C, Greilich S. Methodological accuracy of image-based electron density assessment using dual-energy computed tomography. *Med Phys.* 2017;44(6):2429-2437. https://doi.org/10.1002/mp.12265.
74. Ates O, Hua CH, Zhao L, et al. Feasibility of using post-contrast dual-energy CT for pediatric radiation treatment planning and dose calculation. *Br J Radiol.* 2021;94(1118):20200170.
75. Gjesteby L, De Man B, Jin Y, et al. Metal artifact reduction in CT: where are we after four decades? *IEEE Access*. 2016;4:5826-5849. https://doi.org/10.1109/ACCESS.2016.2608621.
76. Andersson KM, Nowik P, Persliden J, Thunberg P, Norrman E. Metal artifact reduction in CT imaging of hip prostheses-an evaluation of commercial techniques provided by four vendors. *Br J Radiol.* 2015;88(1052):20140473. https://doi.org/10.1259/bjr.20140473.

77. Son SH, Kang YN, Ryu M-R. The effect of metallic implants on radiation therapy in spinal tumor patients with metallic spinal implants. *Med Dosim.* 2012;37(1):98-107.
78. Maerz M, Koelbl O, Dobler B. Influence of metallic dental implants and metal artifacts on dose calculation accuracy. *Strahlenther Onkol.* 2015;191(3):234-241. https://doi.org/10.1007/s00066-014-0774-2.
79. Shioyama Y, Jang SY, Liu HH, et al. Preserving functional lung using perfusion imaging and intensity-modulated radiation therapy for advanced-stage non-small cell lung cancer. *Int J Radiat Oncol Biol Phys.* 2007;68(5):1349-1358. https://doi.org/10.1016/j.ijrobp.2007.02.015.
80. Rousselle A, Amelot A, Thariat J, et al. Metallic implants and CT artifacts in the CTV area: where are we in 2020? *Cancer Radiother.* 2020;24:658-666.
81. Bolstad K, Flatabø S, Aadnevik D, Dalehaug I, Vetti N. Metal artifact reduction in CT, a phantom study: subjective and objective evaluation of four commercial metal artifact reduction algorithms when used on three different orthopedic metal implants. *Acta radiol.* 2018;59:1110-1118.
82. Giantsoudi D, De Man B, Verburg J, et al. Metal artifacts in computed tomography for radiation therapy planning: dosimetric effects and impact of metal artifact reduction. *Phys Med Biol.* 2017;62(8):R49-R80. https://doi.org/10.1088/1361-6560/aa5293.
83. Vellarackal AJ, Kaim AH. Metal artefact reduction of different alloys with dual energy computed tomography (DECT). *Sci Rep.* 2021;11(1):1-11. https://doi.org/10.1038/s41598-021-81600-1.
84. Park J, Kim SH, Han JK. Combined application of virtual monoenergetic high keV images and the orthopedic metal artifact reduction algorithm (O-MAR): effect on image quality. *Abdom Radiol.* 2019;44:756-765.
85. Lim P, Barber J, Sykes J. Evaluation of dual energy CT and iterative metal artifact reduction (iMAR) for artifact reduction in radiation therapy. *Australas Phys Eng Sci Med.* 2019;42:1025-1032.
86. Mazur L, Kisielewicz K, Dziecichowicz A, Sapikowska A. Evaluation of usefulness of dual-energy computed tomographys in radiotherapy planning for patients with hip endoprosthesis. *Acta Phys Pol B.* 2019;50(3):349-360. https://doi.org/10.5506/APhysPolB.50.349.
87. Bär E, Schwahofer A, Kuchenbecker S, Häring P. Improving radiotherapy planning in patients with metallic implants using the iterative metal artifact reduction (iMAR) algorithm. *Biomed Phys Eng Express.* 2015;1:025206.
88. Wang T, Ishihara T, Kono A, et al. Application of dual-energy CT to suppression of metal artifact caused by pedicle screw fixation in radiotherapy: a feasibility study using original phantom. *Phys Med Biol.* 2017;62:6226-6245.
89. Côté N, Bedwani S, Carrier JF. Improved tissue assignment using dual-energy computed tomography in low-dose rate prostate brachytherapy for Monte Carlo dose calculation. *Med Phys.* 2016;43(5):2611-2618. https://doi.org/10.1118/1.4947486.
90. Schwahofer A, Bär E, Kuchenbecker S, Grossmann JG, Kachelrieß M, Sterzing F. The application of metal artifact reduction (MAR) in CT scans for radiation oncology by monoenergetic extrapolation with a DECT scanner. *Z Med Phys.* 2015;25(4):314-325. https://doi.org/10.1016/j.zemedi.2015.05.004.
91. Van Elmpt W, Ruysscher DD, van der Salm A, et al. The PET-boost randomised phase II dose-escalation trial in non-small cell lung cancer. *Radiother Oncol.* 2012;104:67-71.
92. Stieb S, Kiser K, van Dijk L, et al. Imaging for response assessment in radiation oncology: current and emerging techniques. *Hematol Oncol Clin North Am.* 2019;34(1):293-306. https://doi.org/10.1016/j.hoc.2019.09.010.
93. Gregoire V, Haustermans K, Geets X, et al. PET-based treatment planning in radiotherapy : a new standard ? *J Nucl Med.* 2007;48(1):68-77.
94. Schmidt MA, Payne GS. Radiotherapy planning using MRI. *Phys Med Biol.* 2015;60:R323-R361.
95. Thorwarth D. Functional imaging for radiotherapy treatment planning: current status and future directions - a review. *Br J Radiol.* 2015;88:1051. https://doi.org/10.1259/bjr.20150056.
96. Kalisz K, Rassouli N, Dhanantwari A, Jordan D, Rajiah P. Noise characteristics of virtual monoenergetic images from a novel detector-based spectral CT scanner. *Eur J Radiol.* 2018;98(11):118-125. https://doi.org/10.1016/j.ejrad.2017.11.005.
97. Joshi M, Langan DA, Sahani DS, et al. Effective atomic number accuracy for kidney stone characterization using spectral CT. *Phys Med Imaging.* 2010;7622(5):76223K. https://doi.org/10.1117/12.844372.
98. Pelgrim GJ, van Hamersvelt RW, Willemink MJ, et al. Accuracy of iodine quantification using dual energy CT in latest generation dual source and dual layer CT. *Eur Radiol.* 2017;27(9):1-9. https://doi.org/10.1007/s00330-017-4752-9.
99. Schieda N, Al-Dandan O, Shabana W, Flood TA, Malone SC. Is primary tumor detectable in prostatic carcinoma at routine contrast-enhanced CT? *Clin Imaging.* 2015;39(4):623-626. https://doi.org/10.1016/j.clinimag.2015.01.008.
100. Yoon SH, Lee JM, Cho JY, et al. Small (≤ 20 mm) pancreatic adenocarcinomas: analysis of enhancement patterns and secondary signs with multiphasic multidetector CT. *Radiology.* 2011;259:442-452.
101. Vinod SK, Jameson MG, Min M, Holloway LC. Uncertainties in volume delineation in radiation oncology: a systematic review and recommendations for future studies. *Radiother Oncol.* 2016;121(2):169-179. https://doi.org/10.1016/j.radonc.2016.09.009.
102. Bekelman JuE, WOlden S, Lee N. Head-and-neck target delineation among radiation oncology residents after a teaching intervention : a prospective. *blinded pilot study. Int J Radiat Oncol Biol Phys.* 2009;73(2):416-423. https://doi.org/10.1016/j.ijrobp.2008.04.028.
103. Jansen EPM, Nijkamp J, Gubanski M, Lind PARM, Verheij M. Interobserver variation of clinical target volume delineation in gastric cancer. *Int J Radiat Oncol Biol Phys.* 2010;77(4):1166-1170. https://doi.org/10.1016/j.ijrobp.2009.06.023.
104. Caravatta L, Macchia G, Mattiucci GC, et al. Inter-observer variability of clinical target volume delineation in radiotherapy treatment of pancreatic cancer: a multi-institutional contouring experience. *Radiat Oncol.* 2014;9:1-9.
105. Choi HJ, Kim YS, Lee SH, et al. Inter- and intra-observer variability in contouring of the prostate gland on planning computed tomography and cone beam computed tomography. *Acta Oncol (Madr).* 2011;50(4):539-546. https://doi.org/10.3109/0284186X.2011.562916.
106. Foroudi F, Haworth A, Pangehel A, et al. Inter-observer variability of clinical target volume delineation for bladder cancer using CT and cone beam CT. *J Med Imaging Radiat Oncol.* 2009;53:100-106.
107. Peulen H, Belderbos JJJ, Guckenberger M, et al. Target delineation variability and corresponding margins of peripheral early stage NSCLC treated with stereotactic body radiotherapy. *Radiother Oncol.* 2015;114(3):361-366. https://doi.org/10.1016/j.radonc.2015.02.011.
108. Lenga L, Czwikla R, Wichmann JL, et al. Dual-energy CT in patients with colorectal cancer: Improved assessment of hypoattenuating liver metastases using noise-optimized virtual monoenergetic imaging. *Eur J Radiol.* 2018;106:184-191.
109. Lohöfer FK, Kaissis GA, Köster FL, et al. Improved detection rates and treatment planning of head and neck cancer using

dual-layer spectral CT. *Eur Radiol*. 2018;28:4925-4931. https://doi.org/10.1007/s00330-018-5511-2.
110. Toepker M, Czerny C, Ringl H, et al. Can dual-energy CT improve the assessment of tumor margins in oral cancer? *Oral Oncol.* 2014;50(3):221-227. https://doi.org/10.1016/j.oraloncology.2013.12.001.
111. Albrecht MH, Scholtz JE, Kraft J, et al. Assessment of an advanced monoenergetic reconstruction technique in dual-energy computed tomography of head and neck cancer. *Eur Radiol.* 2015;25(8):2493-2501. https://doi.org/10.1007/s00330-015-3627-1.
112. Forghani R. Advanced dual-energy CT for head and neck cancer imaging. *Expert Rev Anticancer Ther.* 2015;15:1489-1501.
113. Frellesen C, Kaup M, Wichmann JL, et al. Noise-optimized advanced image-based virtual monoenergetic imaging for improved visualization of lung cancer: comparison with traditional virtual monoenergetic imaging. *Eur J Radiol.* 2016;85:665-672.
114. Noid G, Currey AD, Bergom C, et al. Improvement of breast tumor delineation for preoperative radiation therapy using dual-energy CT. *Int J Radiat Oncol.* 2017;99:E704.
115. Nagayama Y, Tanoue S, Inoue T, et al. Dual-layer spectral CT improves image quality of multiphasic pancreas CT in patients with pancreatic ductal adenocarcinoma. *Eur Radiol.* 2019;30:394–403. https://doi.org/10.1007/s00330-019-06337-y.
116. Ohira S, Yagi M, Iramina H, et al. Treatment planning based on water density image generated using dual-energy computed tomography for pancreatic cancer with contrast-enhancing agent: phantom and clinical study. *Med Phys.* 2018;45:5208-5217.
117. Beer L, Toepker M, Ba-Ssalamah A, et al. Apfaltrer, P. Objective and subjective comparison of virtual monoenergetic vs. polychromatic images in patients with pancreatic ductal adenocarcinoma. *Eur Radiol.* 2019;29:3617–3625. https://doi.org/10.1007/s00330-019-06116-9.
118. Zhang XF, Lu Q, Wu LM, et al. Quantitative iodine-based material decomposition images with spectral CT imaging for differentiating prostatic carcinoma from benign prostatic hyperplasia. *Acad Radiol.* 2013;20:947-956.
119. Benveniste AP, De Castro Faria S, Broering G, et al. Potential application of dual-energy CT in gynecologic cancer: initial experience. *Am J Roentgenol*. 2017;208(3):695-705. https://doi.org/10.2214/AJR.16.16227.
120. Zopfs D, Laukamp KR, Dos Santos DP, et al. Low-keV virtual monoenergetic imaging reconstructions of excretory phase spectral dual-energy CT in patients with urothelial carcinoma: a feasibility study. *Eur J Radiol.* 2019;116:135-143.
121. Lv P, Lin XZ, Chen K, Gao J. Spectral CT in patients with small HCC: investigation of image quality and diagnostic accuracy. *Eur Radiol.* 2012;22:2117-2124.
122. Pettersson E, Bäck A, Björk-Eriksson T, et al. Structure delineation in the presence of metal – A comparative phantom study using single and dual-energy computed tomography with and without metal artifact reduction. *Phys Imaging Rad Oncol.* 2019;9(12):43-49. https://doi.org/10.1016/j.phro.2019.01.001.
123. Kovacs DG, Rechner LA, Appelt AL, et al. Metal artifact reduction for accurate tumor delineation in radiotherapy. *Radiother Oncol.* 2018;126(3):479-486. https://doi.org/10.1016/j.radonc.2017.09.029.
124. Ito R, Iwano S, Shimamoto H, et al. A comparative analysis of dual-phase dual-energy CT and FDG-PET/CT for the prediction of histopathological invasiveness of non-small cell lung cancer. *Eur J Radiol.* 2017;95(5):186-191. https://doi.org/10.1016/j.ejrad.2017.08.010.
125. Oldan J, He M, Wu T, et al. Pilot Study: evaluation of dual-energy computed tomography measurement strategies for positron emission tomography correlation in pancreatic adenocarcinoma. *J Digit Imaging*. 2014;27(6):824-832. https://doi.org/10.1007/s10278-014-9707-y.
126. Ng SP, Cardenas CE, Elhalawani H, et al. Comparison of tumor delineation using dual energy computed tomography versus magnetic resonance imaging in head and neck cancer re-irradiation cases. *Phys Imaging Rad Oncol.* 2020;14(3):1-5. https://doi.org/10.1016/j.phro.2020.04.001.
127. Sudarski S, Hagelstein C, Weis M, Schoenberg SO, Apfaltrer P. Dual-energy snap-shot perfusion CT in suspect pulmonary nodules and masses and for lung cancer staging. *Eur J Radiol.* 2015;84(12):2393-2400. https://doi.org/10.1016/j.ejrad.2015.09.024.
128. Lenga L, Czwikla R, Wichmann JL, et al. Dual-energy CT in patients with abdominal malignant lymphoma: impact of noise-optimised virtual monoenergetic imaging on objective and subjective image quality. *Clin Radiol.* 2018;73:833.e19-833.e27.
129. Dong Y, Zheng S, Machida H, et al. Differential diagnosis of osteoblastic metastases from bone islands in patients with lung cancer by single-source dual-energy CT: advantages of spectral CT imaging. *Eur J Radiol.* 2015;84(5):901-907. https://doi.org/10.1016/j.ejrad.2015.01.007.
130. Karino T, Ohira S, Kanayama N, et al. Determination of optimal virtual monochromatic energy level for target delineation of brain metastases in radiosurgery using dual energy CT. *Br J Radiol.* 2020;93:1-7.
131. Shi JW, Dai HZ, Shen L, Xu DF. Dual-energy CT: clinical application in differentiating an adrenal adenoma from a metastasis. *Acta Radiol*. 2014;55:505-512.
132. Xie ZY, Chai RM, Ding GC, et al. T and N staging of gastric cancer using dual-source computed tomography. *Gastroenterol Res Pract.* 2018:2018:1–10.
133. Shimamoto H, Iwano S, Umakoshi H, Kawaguchi K, Naganawa S. Evaluation of locoregional invasiveness of small-sized non-small cell lung cancers by enhanced dual-energy computed tomography. *Cancer Imaging*. 2016;16(1):1-8. https://doi.org/10.1186/s40644-016-0077-1.
134. Rössler O, Betge J, Harbaum L, Mrak K, Tschmelitsch J, Langner C. Tumor size, tumor location, and antitumor inflammatory response are associated with lymph node size in colorectal cancer patients. *Mod Pathol.* 2017;30(6):897-904. https://doi.org/10.1038/modpathol.2016.227.
135. Shen C, Liu Z, Wang Z, et al. Building CT radiomics based nomogram for preoperative esophageal cancer patients lymph node metastasis prediction. *Transl Oncol.* 2018;11(3):815-824. https://doi.org/10.1016/j.tranon.2018.04.005.
136. Chong A, Ha JM, Han YH, et al. Preoperative lymph node staging by FDG PET/CT with contrast enhancement for thyroid cancer: a multicenter study and comparison with neck CT. *Clin Exp Otorhinolaryngol.* 2017;10(1):121-128. https://doi.org/10.21053/ceo.2015.01424.
137. Rizzo S, Radice D, Femia M, et al. Metastatic and non-metastatic lymph nodes: quantification and different distribution of iodine uptake assessed by dual-energy CT. *Eur Radiol*. 2018;28:760-769 doi:10.1007/s00330-017-5015-5.
138. Martin SS, Czwikla R, Wichmann JL, et al. Dual-energy CT-based iodine quantification to differentiate abdominal malignant lymphoma from lymph node metastasis. *Eur J Radiol.* 2018;105:255-260.
139. Zeng YR, Yang QH, Liu QY, et al. Dual energy computed tomography for detection of metastatic lymph nodes in patients with hepatocellular carcinoma. *World J Gastroenterol.* 2019;25:1986-1996.
140. Tawfik AM, Razek AA, Kerl JM, Nour-Eldin NE, Bauer R, Vogl TJ. Comparison of dual-energy CT-derived iodine content and iodine overlay of normal, inflammatory and metastatic squamous cell carcinoma cervical lymph nodes. *Eur Radiol.* 2014;24(3):574-580. https://doi.org/10.1007/s00330-013-3035-3.

141. Foust AM, Ali RM, Nguyen XV, et al. Dual-energy CT-derived iodine content and spectral attenuation analysis of metastatic versus nonmetastatic lymph nodes in squamous cell carcinoma of the *oropharynx. Tomography.* 2018;4:2-7.
142. Kraft M, Ibrahim M, Spector M, Forghani R, Srinivasan A. Comparison of virtual monochromatic series, iodine overlay maps, and single energy CT equivalent images in head and neck cancer conspicuity. *Clin Imaging.* 2018;48:26-31.
143. Pan Z, Pang L, Ding B, et al. Gastric cancer staging with dual energy spectral CT imaging. *PLoS One.* 2013;8:17-22.
144. Yang Z, Zhang X, Fang M, et al. Preoperative diagnosis of regional lymph node metastasis of colorectal cancer with quantitative parameters from dual-energy CT. *AJR Am J Roentgenol*. 2019;213(1):W17-W25.
145. Liu X, Ouyang D, Li H, et al. Papillary thyroid cancer: dual-energy spectral CT quantitative parameters for preoperative diagnosis of metastasis to the cervical lymph nodes. *Radiology.* 2015;275:167-176.
146. Al-Najami I, Lahaye MJ, Beets-Tan R,G,H, Baatrup G. Dual-energy CT can detect malignant lymph nodes in rectal cancer. *Eur J Radiol.* 2017;90:81-88.
147. Wu H, Dong S, Li X, et al. Clinical utility of dual-energy CT used as an add-on to 18F FDG PET/CT in the preoperative staging of resectable NSCLC with suspected single osteolytic metastases. *Lung Cancer.* 2020;140:80-86.
148. Kuno H, Onaya H, Fujii S, Ojiri H, Otani K, Satake M. Primary staging of laryngeal and hypopharyngeal cancer: CT, MR imaging and dual-energy CT. *Eur J Radiol.* 2014;83:e23–e35.
149. Brouwer CL, Steenbakkers RJHM, Heuvel EVD, Duppen JC, Navran A. 3D Variation in delineation of head and neck organs at risk 3D variation in delineation of head and neck organs at risk. *Radiat Oncol*. 2012;7:32.
150. Wang C, Zhu X, Hong JC, Zheng D. Artificial intelligence in radiotherapy treatment planning: present and future. *Technol Cancer Res Treat*. 2019;18:1-11.
151. Michalak G, Grimes J, Fletcher J, et al. Technical Note: improved CT number stability across patient size using dual-energy CT virtual monoenergetic imaging. *Med Phys.* 2016;43:513-517.
152. Hurrell MA, Butler APH, Cook NJ, Butler PH, Ronaldson JP, Zainon R. Spectral Hounsfield units: a new radiological concept. *Eur Radiol.* 2012;22:1008-1013.
153. Chen S, Zhong X, Hu S, et al. Automatic multi-organ segmentation in dual-energy CT (DECT) with dedicated 3D fully convolutional DECT networks. *Med Phys.* 2020;47:552-562.
154. Sánchez JCG, Magnusson M, Sandborg M. Segmentation of bones in medical dual-energy computed tomography volumes using the 3D U-Net. *Phys Med*. 2020;69:241-247.
155. van der Heyden B, Wohlfahrt P, Eekers DBP, et al. Dual-energy CT for automatic organs-at-risk segmentation in brain-tumor patients using a multi-atlas and deep-learning approach. *Sci Rep.* 2019;9:4126 https://doi.org/10.1038/s41598-019-40584-9.
156. Wang T, Ghavidel BB, Beitler JJ, et al. Optimal virtual monoenergetic image in "TwinBeam" dual-energy CT for organs-at-risk delineation based on contrast-noise-ratio in head-and-neck radiotherapy. *J Appl Clin Med Phys.* 2019;20:121-128.
157. Matuszak MM, Kashani R, Green M, Owen D, Jolly S, Mierzwa M. Functional adaptation in radiation therapy. *Semin Radiat Oncol.* 2019;29(3):236-244. https://doi.org/10.1016/j.semradonc.2019.02.006.
158. Ling CC, Humm J, Larson S, et al. Towards multidimensional radiotherapy (MD-CRT): biological imaging and biological conformality. *Int J Radiat Oncol Biol Phys.* 2000;47:551-560.
159. Groenendaal G, Moman MR, Korporaal JG, et al. Validation of functional imaging with pathology for tumor delineation in the prostate. *Radiother Oncol.* 2010;94:145-150.
160. Bentzen SM. Theragnostic imaging for radiation oncology: dose-painting by numbers. *Lancet Oncol*. 2005;6:112-117.
161. Cao Y. The promise of dynamic contrast-enhanced imaging in radiation therapy. *Semin Radiat Oncol.* 2011;21:147-156.
162. O'Connor JPB, Tofts PS, Miles KA, Parkes LM, Thompson G, Jackson A. Dynamic contrast-enhanced imaging techniques: CT and MRI. *Br J Radiol.* 2011;84:S112-S120.
163. Osimani M, Bellini D, Di Cristofano C, et al. Perfusion MDCT of prostate cancer: correlation of perfusion CT parameters and immunohistochemical markers of angiogenesis. *Am J Roentgenol.* 2012;199(5):1042-1048. https://doi.org/10.2214/AJR.11.8267.
164. Elmpt WV, Das M, Hüllner M, et al. Characterization of tumor heterogeneity using dynamic contrast enhanced CT and FDG-PET in non-small cell lung cancer. *Radiother Oncol.* 2013;109:65-70.
165. Thaiss WM, Sauter AW, Bongers M, et al. Clinical applications for dual energy CT versus dynamic contrast enhanced CT in oncology. *Eur J Radiol.* 2015;84(12):2368-2379. https://doi.org/10.1016/j.ejrad.2015.06.001.
166. Iwano S, Ito R, Umakoshi H, Ito S, Naganawa S. Evaluation of lung cancer by enhanced dual-energy CT: association between three-dimensional iodine concentration and tumor differentiation. *Br J Radiol.* 2015;88:1055. https://doi.org/10.1259/bjr.20150224.
167. Lin L, Cheng J, Tang D, et al. The associations among quantitative spectral CT parameters, Ki-67 expression levels and EGFR mutation status in NSCLC. *Sci Rep.* 2020;10:3436. https://doi.org/10.1038/s41598-020-60445-0.
168. Tang W, Wu N, Huang Y, Wang Y, Niu L. Correlation between clinicopathological features and spectral CT imaging of lung squamous cell carcinoma. *Adv Ultrasound Diagn Ther.* 2020;4:9-17. https://doi.org/10.37015/AUDT.2020.190027.
169. Li X, Meng X, Ye Z. Iodine quantification to characterize primary lesions, metastatic and non-metastatic lymph nodes in lung cancers by dual energy computed tomography: an initial experience. *Eur J Radiol.* 2016;85:1219-1223.
170. Li Y, Li X, Ren X, Ye Z. Assessment of the aggressiveness of rectal cancer using quantitative parameters derived from dual-energy computed tomography. *Clin Imaging.* 2020;68:136-142.
171. Schmid-Bindert G, Henzler T, Chu TQ, et al. Functional imaging of lung cancer using dual energy CT: how does iodine related attenuation correlate with standardized uptake value of 18FDG-PET-CT? *Eur Radiol.* 2012;22:93-103.
172. Yaremenko S, Sinitsyn V, Ruchiova N, Mershina EA. Comparison of the Dual Energy-Computed Tomography (DECT) with PET-CT for Tissue Characterisation in Lung Cancer. European Society of Radiology; 2019.
173. Tanaka M, Koji I, Fujioka I, et al. Impact of low iodine density tumor area ratio on the local control of non-small cell lung cancer through stereotactic body radiotherapy. *J Radiat Res.* 2021;62:448-456.
174. Marcus CD, Ladam-Marcus V, Cucu C, Bouché O, Lucas L, Hoeffel C. Imaging techniques to evaluate the response to treatment in oncology: current standards and perspectives. *Crit Rev Oncol Hematol.* 2009;72:217-238.
175. Padhani AR, Khan AA. Diffusion-weighted (DW) and dynamic contrast-enhanced (DCE) magnetic resonance imaging (MRI) for monitoring anticancer therapy. *Target Oncol.* 2010;5:39-52.
176. Rasmussen F, Madsen HHT. Imaging follow-up of RF ablation of lung tumors. *Cancer Imaging.* 2011;11:123-128.
177. Bellomi M, Petralia G, Sonzogni A, Zampino MG, Rocca A. CT perfusion for the monitoring of neoadjuvant chemotherapy and radiation therapy in rectal carcinoma: initial experience. *Radiology.* 2007;244:486–493.
178. De Lussanet QG, Backes WH, Griffioen AW, et al. Dynamic contrast-enhanced magnetic resonance imaging of radiation therapy-induced microcirculation changes in rectal cancer. *Int J Radiat Oncol Biol Phys.* 2005;63:1309-1315.
179. Kim SH, Lee JM, Gupta SN, Han JK, Choi BI. Dynamic contrast-enhanced MRI to evaluate the therapeutic response to

neoadjuvant chemoradiation therapy in locally advanced rectal cancer. *J Magn Reson Imaging.* 2014;40:730-737.
180. Sawyer B, Pun E, Samuel M, et al. CT perfusion imaging in response assessment of pulmonary metastases undergoing stereotactic ablative radiotherapy. *J Med Imaging Radiat Oncol.* 2015;59:207-215.
181. Tacelli N, Santangelo T, Scherpereel A, et al. Perfusion CT allows prediction of therapy response in non-small cell lung cancer treated with conventional and anti-angiogenic chemotherapy. *Eur Radiol.* 2013;23:2127-2136.
182. Mayr NA, Wang JZ, Zhang D, et al. Longitudinal changes in tumor perfusion pattern during the radiation therapy course and its clinical impact in cervical cancer. *Int J Radiat Oncol Biol Phys.* 2010;77:502-508.
183. Zahra MA, Tan LT, Priest AN, et al. Semiquantitative and quantitative dynamic contrast-enhanced magnetic resonance imaging measurements predict radiation response in cervix cancer. *Int J Radiat Oncol Biol Phys.* 2009;74:766-773.
184. Li XS, Fan HX, Zhu HX, Song YL, Zhou CW. The value of perfusion CT in predicting the short-term response to synchronous radiochemotherapy for cervical squamous cancer. *Eur Radiol.* 2012;22:617-624.
185. Hermans R, Meijerink M, Van Den Bogaert W, Rijnders A, Weltens C, Lambin P. Tumor perfusion rate determined noninvasively by dynamic computed tomography predicts outcome in head-and-neck cancer after radiotherapy. *Int J Radiat Oncol Biol Phys.* 2003;57(5):1351-1356. https://doi.org/10.1016/S0360-3016(03)00764-8.
186. Park MS, Klotz E, Kim M-J, et al. Perfusion CT: noninvasive surrogate marker for stratification of pancreatic cancer response to concurrent chemo- and radiation therapy. *Radiology.* 2009;250:110-117.
187. Meyer M, Hohenberger P, Apfaltrer P, et al. CT-based response assessment of advanced gastrointestinal stromal tumor: dual energy CT provides a more predictive imaging biomarker of clinical benefit than RECIST or Choi criteria. *Eur J Radiol.* 2013;82:923-928.
188. Schramm N, Schlemmer M, Englhart E, et al. Dual energy CT for monitoring targeted therapies in patients with advanced gastrointestinal stromal tumor: initial results. *Curr Pharm Biotechnol.* 2011;12:547-557.
189. Kim WW, Lee CH, Goo JM, et al. Xenon-enhanced dual-energy CT of patients with asthma: dynamic ventilation changes after methacholine and salbutamol inhalation. *Am J Roentgenol.* 2012;199:975-981.
190. Hwang SH, Yoo MR, Park CH, Jeon TJ, Kim SJ, Kim TH. Dynamic contrast-enhanced CT to assess metabolic response in patients with advanced non-small cell lung cancer and stable disease after chemotherapy or chemoradiotherapy. *Eur Radiol.* 2013;23:1573-1581.
191. Jiang C, Yang P, Lei J, et al. The application of iodine quantitative information obtained by dual-source dual-energy computed tomography on chemoradiotherapy effect monitoring for cervical cancer. *J Comput Assist Tomogr.* 2017;41(5):737-745
192. Noid G, Tai A, Schott D, et al. Enhancing soft tissue contrast and radiation induced image changes with dual-energy CT for radiation therapy. *Med Phys.* 2016. https://doi.org/10.1002/mp.13083.
193. Bahig H, Lapointe A, Bedwani S, et al. Dual-energy computed tomography for prediction of loco-regional recurrence after radiotherapy in larynx and hypopharynx squamous cell carcinoma. *Eur J Radiol.* 2019;110:1-6.
194. Preda L, Calloni SF, Moscatelli MEM, Cossu Rocca M, Bellomi M. Role of CT perfusion in monitoring and prediction of response to therapy of head and neck squamous cell carcinoma. *Biomed Res Int.* 2014;2014:917150.
195. Ren Y, Jiao Y, Ge W, et al. Dual-energy computed tomography-based iodine quantitation for response evaluation of lung cancers to chemoradiotherapy/radiotherapy: a comparison with fluorine-18 fluorodeoxyglucose positron emission tomography/computed tomography-based positron emission. *J Comput Assist Tomogr.* 2018;42:614-622.
196. Baxa JAN, Ludvik J, Sedlmair M, Flohr T, Schmidt B. Correlation of Iodine Quantification and FDG Uptake in Early Therapy Response Assessment of Non-small Cell Lung Cancer: Possible Benefit of Dual-energy CT Scan as an Integral Part of PET / CT Examination. 2020;3468:3459-3468. https://doi.org/10.21873/anticanres.14332
197. Sauter AP, Kössinger A, Beck S, et al. Dual-energy CT parameters in correlation to MRI-based apparent diffusion coefficient: evaluation in rectal cancer after radiochemotherapy. *Acta Radiol Open*. 2020;9(9):2058460120945316. https://doi.org/10.1177/2058460120945316.
198. Fehrenbach U, Feldhaus F, Kahn J, et al. Tumor response in non-small-cell lung cancer patients treated with chemoradiotherapy – Can spectral CT predict recurrence? *J Med Imaging Radiat Oncol.* 2019;63:641-649.
199. Munawar I, Yaremko BP, Craig J, et al. Intensity modulated radiotherapy of non-small-cell lung cancer incorporating SPECT ventilation imaging. *Med Phys.* 2010;37(4):1863-1872. https://doi.org/10.1118/1.3358128.
200. Siva S, Thomas R, Callahan J, et al. High-resolution pulmonary ventilation and perfusion PET/CT allows for functionally adapted intensity modulated radiotherapy in lung cancer. *Radiother Oncol.* 2015;115(2):157-162. https://doi.org/10.1016/j.radonc.2015.04.013.
201. Bahig H, Campeau MP, Lapointe A, et al. Phase 1-2 study of dual-energy computed tomography for assessment of pulmonary function in radiation therapy planning. *Int J Radiat Oncol Biol Phys*. 2017;99(2):334-343. https://doi.org/10.1016/j.ijrobp.2017.05.051.
202. Yamamoto T, Kabus S, Lorenz C, et al. 4D CT lung ventilation images are affected by the 4D CT sorting method. *Med Phys.* 2013;40(10):101907. https://doi.org/10.1118/1.4820538.
203. Tajik JK, Tran BQ, Hoffman EA. Xenon enhanced CT imaging of local pulmonary ventilation. *Proc SPIE*. 1996;2709:40–54.
204. Ohno Y, Yoshikawa T, Takenaka D, et al. Xenon-enhanced CT using subtraction CT: basic and preliminary clinical studies for comparison of its efficacy with that of dual-energy CT and ventilation SPECT/CT to assess regional ventilation and pulmonary functional loss in smokers. *Eur J Radiol.* 2017;86:41-51.
205. Eun JC, Seo JB, Goo HW, et al. Xenon ventilation CT with a dual-energy technique of dual-source CT: initial experience. *Radiology.* 2008;248:615-624.
206. Acuff SN, Jackson AS, Subramaniam RM, Osborne D. Practical considerations for integrating PET /CT into radiation therapy planning. *J Nucl Med Technol.* 2018;46(4):343-349. https://doi.org/10.2967/jnmt.118.209452.
207. Hwang HJ, Lee SMSW, Seo JB, et al. Assessment of changes in regional xenon-ventilation, perfusion, and ventilation-perfusion mismatch using dual-energy computed tomography after pharmacological treatment in patients with chronic obstructive pulmonary disease: visual and quantitative analysis. *Int J Chron Obstruct Pulmon Dis.* 2019;14:2195-2203. https://doi.org/10.2147/copd.s210555.
208. Aoki K, Izumi Y, Watanabe W, et al. Generation of ventilation/perfusion ratio map in surgical patients by dual-energy CT after xenon inhalation and intravenous contrast media. *J Cardiothor Surg.* 2018;13(1):1-10. https://doi.org/10.1186/s13019-018-0737-2.
209. Sauter A, Hammel J, Ehn S, et al. Perfusion-ventilation CT via three-material differentiation in dual-layer CT: a feasibility study. *Eur Radiol.* 2019;9:1-8.
210. Ohira S, Kanayama N, Toratani M, Ueda Y, Koike Y. Stereotactic body radiation therapy planning for liver tumors using

functional images from dual-energy computed tomography. *Radiother Oncol*. 2020;145:56–62. https://doi.org/10.1016/j.radonc.2019.12.002.
211. Odisio EG, Truong MT, Duran C, de Groot PM, Godo MC. Role of dual-energy computed tomography in thoracic oncology. *Radiol Clin North Am.* 2018;56:535-548.
212. De Cecco CN, Darnell A, Rengo M, et al. Dual-energy CT: oncologic applications. *AJR Am J Roentgenol*. 2012;199:98-105.
213. Atwi NE, Sabottke CF, Pitre DM, Smith DL. Follow-up recommendation rates associated with spectral detector dual-energy CT of the abdomen and pelvis : a retrospective comparison to single-energy CT. *J Am Coll Radiol.* 2020;17:940-950. https://doi.org/10.1016/j.jacr.2019.12.029.
214. Megibow AJ. Clinical abdominal dual - energy CT : 15 years later. *Abdom Radiol.* 2020;45:1198-1201.
215. Moghanaki D, Turkbey B, Vapiwala N, et al. Advances in prostate cancer MRI and PET/CT for staging and radiotherapy treatment planning. *Semin Radiat Oncol*. 2018;27:21-33.
216. van der Heide UA, Houweling AC, Groenendaal G, Beets-Tan RGHH, Lambin P. Functional MRI for radiotherapy dose painting. *Magn Reson Imaging.* 2012;30(9):1216-1223. https://doi.org/10.1016/j.mri.2012.04.010.
217. Vogel WV, Lam MGEH, Pameijer FA, et al. Functional imaging in radiotherapy in the Netherlands: availability and impact on clinical practice. *Clin Oncol.* 2016;28(12):e206-e215. https://doi.org/10.1016/j.clon.2016.09.003.
218. Choudhury A, Budge G, MacKay R, et al. The future of image-guided radiotherapy. *Clin Oncol.* 2017;29:662-666.
219. Winkel D, Bol GH, Kroon PS, et al. Adaptive radiotherapy: the Elekta unity MR-linac concept. *Clin Transl Radiat Oncol.* 2019;18:54-59.
220. Maspero M, Seevinck PR, Schubert G, et al. Quantification of confounding factors in MRI-based dose calculations as applied to prostate IMRT. *Phys Med Biol.* 2017;62:948-965.
221. Edmund JM, Nyholm T. A review of substitute CT generation for MRI-only radiation therapy. *Radiat Oncol*. 2017;12(1):1-15. https://doi.org/10.1186/s13014-016-0747-y.
222. Persson E, Gustafsson CJ, Ambolt P, et al. MR-PROTECT : clinical feasibility of a prostate MRI-only radiotherapy treatment workflow and investigation of acceptance criteria. *Rad Oncol*. 2020;15:77.
223. Pollard JM, Wen Z, Sadagopan R, Wang J. The future of image-guided radiotherapy will be MR guided. *Br J Radiol*. 2017;90:20160667
224. Sjöblom O, Turnbull-Smith S, Minn H, Keyriläinen J. Comparison of cost and time effectiveness between CT- and MRI-based radiotherapy workflow for prostate cancer. In: Cacace M, ed. *Well-Being in the Information Society. Fruits of Respect*. Springer; 2020. https://doi.org/10.1007/978-3-030-57847-3_4.
225. Herk MV, Mcwilliam A, Dubec M, Faivre-finn C, Choudhury A. Magnetic resonance imaging-guided radiation therapy : a short strengths, weaknesses, opportunities, and threats analysis. *Radiat Oncol Biol.* 2018;101:1057-1060.
226. Hoeben BAW, Bussink J, Troost EGC, et al. *Molecular PET imaging for biology-guided adaptive radiotherapy of head and neck cancer. Acta Oncol.* 2013;52:1257–1271. https://doi.org/10.3109/0284186X.2013.812799.
227. van Velden FHP, Kramer GM, Frings V, et al. Repeatability of radiomic features in non-small-cell lung cancer [18F]FDG-PET/CT studies: impact of reconstruction and delineation. *Mol Imaging Biol.* 2016;18:788-795.
228. Kim H, Goo JM, Kang CK. Comparison of iodine density measurement among dual-energy computed tomography scanners from 3 vendors. *Invest Radiol*. 2018;53:321-327.
229. Sheng K. Artificial intelligence in radiotherapy: a technological review. *Front Med.* 2020;14:431-449. https://doi.org/10.1007/s11684-020-0761-1.
230. Su K, Kuo J-W, Jordan DW, et al. Machine learning-based dual-energy CT parametric mapping. *Phys Med Biol*. 2018;63:125001.
231. Shapira N, Fokuhl J, Schultheiß M, et al. Benefit of dual energy CT for lesion localization and classification with convolutional neural networks. Paper presented at: Proceeding of SPIE Medical Imaging; March 16, 2020; Houston, TX. https://doi.org/10.1117/12.2549291.
232. Li J, Dong D, Fang M, et al. Dual-energy CT–based deep learning radiomics can improve lymph node metastasis risk prediction for gastric cancer. *Eur Radiol.* 2020;30:2324-2333. https://doi.org/10.1007/s00330-019-06621-x.
233. Shiraishi Y, Yamada Y, Tanaka T, et al. Single-energy metal artifact reduction in postimplant computed tomography for I-125 prostate brachytherapy: Impact on seed identification. *Brachytherapy*. 2016;15(6):768-773. https://doi.org/10.1016/j.brachy.2016.07.006.
234. Kim YN, Lee HY, Lee KS, et al. Dual-energy CT in patients treated with anti-angiogenic agents for non-small cell lung cancer: new method of monitoring tumor response? *Korean J Radiol.* 2012;13:702-710.
235. Andersson KM, Norrman E, Geijer H, et al. Visual grading evaluation of commercially available metal artifact reduction techniques in hip prosthesis computed tomography. *Br J Radiol.* 2016;89:20150993.

How to cite this article: Kruis MF. Improving radiation physics, tumor visualisation, and treatment quantification in radiotherapy with spectral or dual-energy CT. *J Appl Clin Med Phys*. 2022;23:e13468. https://doi.org/10.1002/acm2.13468